Structure of Turbulent Shear Flows

By A.K.M.F. HUSSAIN[1], J. JEONG[1] AND J. KIM[2]

Introduction

The accuracy and spatial resolution of numerically simulated databases for turbulent shear flows, like those generated at NASA/Ames, far exceed those typically available in laboratory experiments. While there are limitations of the simulations, in particular regarding low Reynolds number (a technological constraint) and limited duration of flow that can be computed (an economic constraint), the simulations have also the advantage that they enable the scientists to "measure" quantities (such as enstrophy, pressure, dissipation, helicity, and pressure-strain rate correlation) which are virtually impossible to measure accurately in the laboratory (see Hussain, 1983, 1986). Simulations provide quantitative measures of flow fields free from the effects of probe interference and from errors introduced by invoking Taylor's hypothesis. The simulations thus accord heretofore unavailable unique opportunities for research into the structure of turbulence; such was our goal and the centerpiece of our effort during the 1987 summer school of Stanford-NASA CTR.

Our research covered three different topics:

(1) Eduction of coherent structures,
(2) Measurement of propagation velocities of perturbations (such as velocity, pressure, and vorticity) in turbulent shear flows, and
(3) Direct evaluation of the Taylor hypothesis.

In the following, we summarize our activities during the summer school in each of these three categories. However, most of our effort was devoted to item (1), which will occupy the bulk of this report. Recognizing that very little time was available to either complete the post-processing or to even adequately digest the results obtained, we venture to point out a few apparent interesting observations and surprises, make some tentative conclusions and suggest specific areas of continuing collaboration between NASA-Ames and University of Houston.

A. Eduction of coherent structures

Coherent structures, an embodiment of our search for order in disorder, has been the focus of much of the research in turbulent shear flows in the past two decades. The overwhelming majority of coherent structure studies has been based on flow visualization, which is not only qualitative but can even be grossly misleading (Hussain, 1986). We need hard quantitative data regarding the distributions of properties over the spatial extent of the structures and the dynamical roles of these

1 University of Houston
2 NASA-Ames Research Center

structures. These structures being defined in terms of coherent vorticity (Hussain, 1980), the requirement of vorticity measurement presents a severe constraint. A first simplification of this problem was to measure one component of vorticity only and in one plane only—that in the azimuthal plane. The initial approach was to perform phase-locked measurements triggered on the periodicity of the flow event or of a forcing signal (Cantwell & Coles, 1983; Hussain & Zaman, 1980; Hussain, Kleis & Sokolov, 1980). Note that structures in natural (unexcited) shear flows undergo jitters of two kinds: initiation and evolutionary jitters. Via excitation, initiation of structure formation can be controlled, but the evolutionary jitter remains uncontrolled. Thus eduction, even in periodically induced structures, must use a local trigger at the measurement location instead of an upstream trigger—a major drawback of Cantwell & Coles' data.

The next step was to develop a scheme for eduction of coherent structures in an unexcited flow by using a local footprint of passing structures (Zaman & Hussain, 1984). In parallel, efforts were devoted to develop an algorithm that can educe structures in any fully developed turbulent flow without requiring any trigger signal. This resulted in a scheme which utilizes the measurement signal itself. Such a technique (to be explained below) was first developed for eduction of structures in the fully developed region of an axisymmetric jet (Tso, 1983) and was further refined to educe structures in a turbulent plane wake (Hayakawa & Hussain, 1985). This generic and robust scheme, which can be applied to data in any transitional and turbulent shear flow, was also successfully applied to numerical simulation and experimental data in a plane mixing layer (Metcalfe et al., 1985). The close agreement between structures educed from numerical and experimental data is strong evidence of the robustness of the scheme as well as a validation of the simulation.

Our goal in this area continues to be: (i) eduction of coherent structure topology in different turbulent flows, (ii) understanding of turbulence phenomena in terms of entrainment, mixing, production, and dissipation, and (iii) the dynamical role and significance of coherent structures in various turbulent shear flows. This provides the motivation for eduction of coherent structures from direct simulations of turbulent flows. While the coherent structure topology and dynamics in the wall region of a turbulent boundary layer would not be expected to be different from those in the wall region of a channel, the outer layer structures must be noticeably different between the two flows. Hence the motivation for studying coherent structures in a flat plate boundary layer and a channel flow. These new data would establish how coherent structures in the wall-bounded flows are different from coherent structures in free shear flows, which have been studied extensively at University of Houston. Having decided to especially focus on the coherent structures near the wall, which are responsible for the most interesting events in wall-bounded shear flows, it was necessary to separate the effects of the wall from those of shear. Hence the goal of eduction of coherent structures in homogeneous shear flows.

The simulation data in a low Reynolds number, fully turbulent channel flow (Kim, Moin & Moser, 1987), in a flat plate boundary layer (Spalart, 1987), and in two homogeneous shear flows (Rogers & Moin, 1987; Lee & Reynolds, 1985) are used to

educe coherent structures in these flows.

Eduction methodology:

Even though the eduction procedure, in principle, is based on the 3D vorticity information in a flow field, experimental limitation forced us to implement the procedure on one component of vorticity, namely the spanwise vorticity, ω_z. In order to permit meaningful comparison with experimental data, our earlier eduction from numerical simulation was also based on only the ω_z field of the simulation (Metcalfe et al., 1985).

The eduction procedure is briefly outlined here. Readers can find further details in our earlier papers. The eduction steps are as follows: (i) select a small y-range where coherent structures are to be studied and obtain $\omega_z(x, y)$ data from simulations in various z-planes, but centered at the middle of this y-range (x, y, z are longitudinal, transverse, and spanwise coordinates, respectively); (ii) smooth the $\omega_z(x, y)$ data using a zero-phase shift filter; (iii) detect structures which are strong (i.e., peak vorticity above a threshold ω_{t_1}) and of a sufficiently large size; (iv) look for z-symmetry of these vorticity concentrations; (v) accept ω_z data from a plane of symmetry (being careful not to accept two planes of the same structure).

The phase average of all realizations containing similar structures yields a coherent structure. Note that a coherent structure is a stochastic quantity and may not be observed instantaneously. The center (marked by the peak value) of smoothed ω_z contours is only a first guess, and is a useful reference for initial alignment of various realizations, but may have nothing to do with the true center, which must be determined from the ensemble averaging after proper alignment.

The eduction continues as follows: (vi) align ω_z with respect to the peaks of smoothed contours and obtain the ensemble average — this is the *zeroth iteration ensemble average* Ω_0; (vii) obtain cross correlation $R_{\omega_1\Omega_0}$ of each realization with the ensemble average; (viii) shift the center of each realization by the location in (x, y) for peak correlation; (ix) reject realizations requiring excessive shifts; (x) obtain ensemble average of the realizations by aligning them with respect to the new centers—this is the *first iteration ensemble average*; (xi) reject realizations that produce excessively low correlation peaks; (xii) continue the iteration until all shifts required for alignment fall below a size and all correlation peaks are above a set level; (xiii) identify the locations of revised centers of finally accepted realizations in the unsmoothed data records and obtain ensemble average after aligning with respect to these centers—this final ensemble average is the coherent structure; (xiv) the departure of each *unsmoothed* realization from the ensemble average denotes incoherent turbulence.

In the eduction, we set ω_{t_1} in terms of the local maximum of mean $\omega_z(y)$. In case of the channel flow, the structures educed were those centered at $y^+ = 125$, 50, 30, and 15.

The educed velocity vector patterns in the (x, y)-plane for the four locations are shown in Figs. 1(a-d). All the four contours show some similarities, characterized by saddles and centers. We had anticipated the structure at $y^+ = 125$ (note $y^+ = 180$ at the centerline of the channel) to resemble to some extent the mixing layer structure

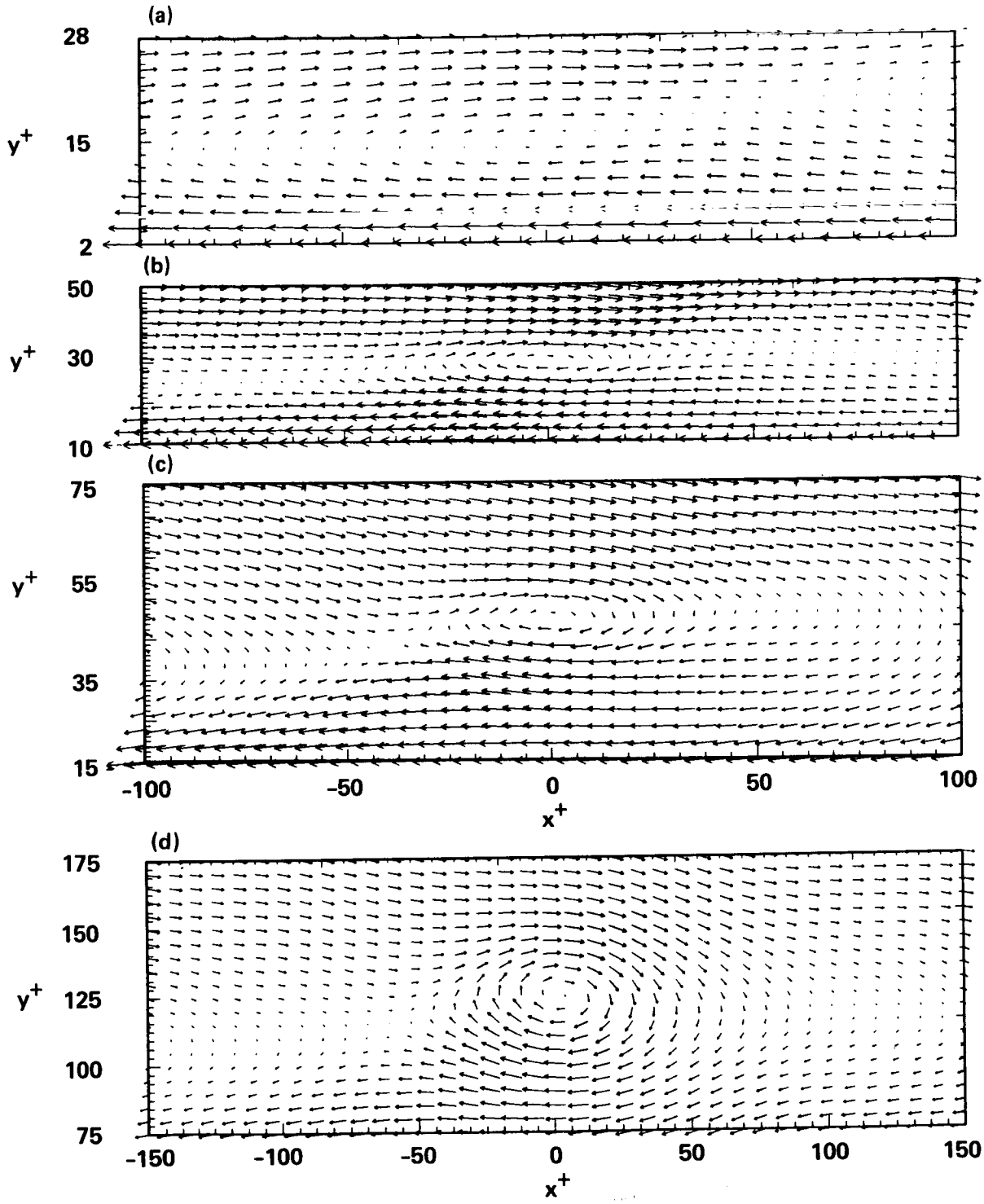

FIGURE 1. Educed velocity vector patterns in (x, y)-plane: (a) Centered at $y^+ = 15$; (b) $y^+ = 30$; (c) $y^+ = 50$; (d) $y^+ = 125$. Note that the y-scales are stretched at different factors for each figures.

studied extensively before (see Hussain & Zaman, 1985; Metcalfe et al., 1985), but the near wall structures appear to be different presumably due to the effects of the wall and high shear. For this reason we present detailed data for structures centered at both $y^+ = 125$ and $y^+ = 15$. The results for $y^+ = 15$ are presented in Figs. 2(a-m) as contours of coherent vorticity $< \omega_z >$; coherent longitudinal and transverse velocities $< u >$ and $< v >$; coherent pressure $< p >$; incoherent turbulent kinetic energy $< q_r^2 >$; incoherent Reynolds stress $-< u_r v_r >$; incoherent pressure $< p_r^2 >$; coherent strain rate $< S >=< \partial u/\partial y > + < \partial v/\partial x >$; coherent shear production $< P_S >= - < u_r v_r >< S >$; coherent normal production $< P_N >= - < u_r^2 > \partial < u > /\partial x - < v_r^2 > \partial < v > /\partial y$; total production $< P_T >=< P_S > + < P_N >$; coherent pressure works $< p >< S_{11} >$, $< p >< S_{22} >$. Note that the y-scale is expanded relative to the x-scale in order to reveal the details of the flow field and that two vorticity contours are duplicated in all figures to provide a common reference. The corresponding contours for $y^+ = 125$ in the channel flow are shown in Figs. 3(a-m).

We have started educing structures at four transverse locations in the Spalart's boundary layer as well as one location each in the homogeneous shear flows. For the purposes of this preliminary report, we limit our discussions primarily to the case of channel structures centered at $y^+ = 15$.

In the frame of the advected coherent structure, the flow above it moves downstream and the flow below it moves upstream. The structure advection velocity being about 60% of the centerline velocity, the downstream stagnation point is closer to it than the upstream one. One would thus expect the normal production at the front to be higher than at the back, as is indeed the case (Fig. 3j). Note that nearer to the center of the channel, the shear is weak and more nearly uniform across the structure. That is why the two saddles are nearly equidistant from the center, and the normal productions are equal on both the front and the back.

The coherent pressure contour extends in the transverse direction considerably beyond the structure boundary as denoted by coherent vorticity. This is to be expected from the fact that pressure is an integral property, being the solution of a Poisson equation with the source term due to gradients of the velocity field. Note that the minimum of coherent pressure is at around the structure center, but does not exactly coincide with it.

One striking feature is the fact that longitudinal pressure work is mostly negative (hence of the right sign) at $y^+ = 125$ but mostly positive at $y^+ = 15$ (hence of the wrong sign). That is, the pressure work transfers kinetic energy away from the longitudinal component in the outer layer as is commonly presumed on the basis of time average kinetic energy balance (see Tennekes & Lumley, 1972), and it transfers kinetic energy into the longitudinal component (contrary to expectation) near the wall. This is consistent with the result of Moin & Kim (1982), in which they attributed it to the "splatting"motions of large eddies in the near-wall region.

Since the shear layer below the advecting structure (near the wall) has a higher velocity gradient than the one above the structure (toward the centerline), one would expect the shear production $< P_S >$ to be higher on the left- than on the

right-hand side of the structure. Data show the two regions to have comparable levels of $< P_S >$, suggesting that the incoherent Reynolds stress $< u_r v_r >$ is higher at the top right-hand side of the structure. Note that both $< P_N >$ and $< P_S >$ are coordinate dependent and it is their sum which is invariant under rotation (Hussain, 1983). The total production $< P_T >$ is higher at the top on the right- hand side.

Concluding remarks

The success of the eduction scheme in extracting coherent structure details in the fully turbulent channel flow is demonstrated. In the plane of z-symmetry the coherent structure characteristics are quite similar to those in the free mixing layer—more so in the outer regions than near the wall. The topology consists of saddles and centers, the saddle region being the location of maximum incoherent Reynolds stress $-< u_r v_r >$, and maximum shear production. One interesting difference from the mixing layer case is that the center in the wall-bounded case is not necessarily characterized by a high level of incoherent turbulence intensity.

While we need to devote more time to compare our channel data with those in jets, wakes and shear layers, some of the measures have not been obtained yet in the free shear flows: for example, contours of dissipation, pressure work, etc. These measurements and simulations are planned in the future. One noticeable difference between the educed structures at $y^+ = 125$ and $y^+ = 15$ is that the structure in the former case is more rounded while in the latter case it is much more sheared. In order to determine the role of shear while eliminating any effect of the wall, it would be worthwhile to educe these structures in homogeneous shear flows with different shear rates. This work is in progress now.

While we do not expect any noticeable difference in the near-wall coherent structure characteristics between channel flow and flat plate boundary layer, the outer layer structures can be quite different in the two flows on two accounts. In the boundary layer, the outer structures should all be of the same sign and be bounded by irrotational (nonturbulent) fluid which they entrain. In the case of the channel, the outer region should consist of structures originating from both walls and can be significantly different as a result of interaction of these structures of oppositely-signed circulations.

When all these data are completed, we will be able to identify the similarities and differences among structure topologies in the channel flow, the boundary layer and homogeneous shear flow. We then hope to be able to comment specifically on the role of the nonturbulent freestream, on the role of shear, and on the role of the wall.

Future extensions

We propose to extend this work to include the following:

(1) Starting from the plane of symmetry, march ahead on either side to track the coherent vortical structure and educe structure details in local planes and then reconstruct the three-dimensional structure.

(2) Educe structures with circulation opposite to the direction of mean shear. This is important in the outer region of the channel where structures migrate from

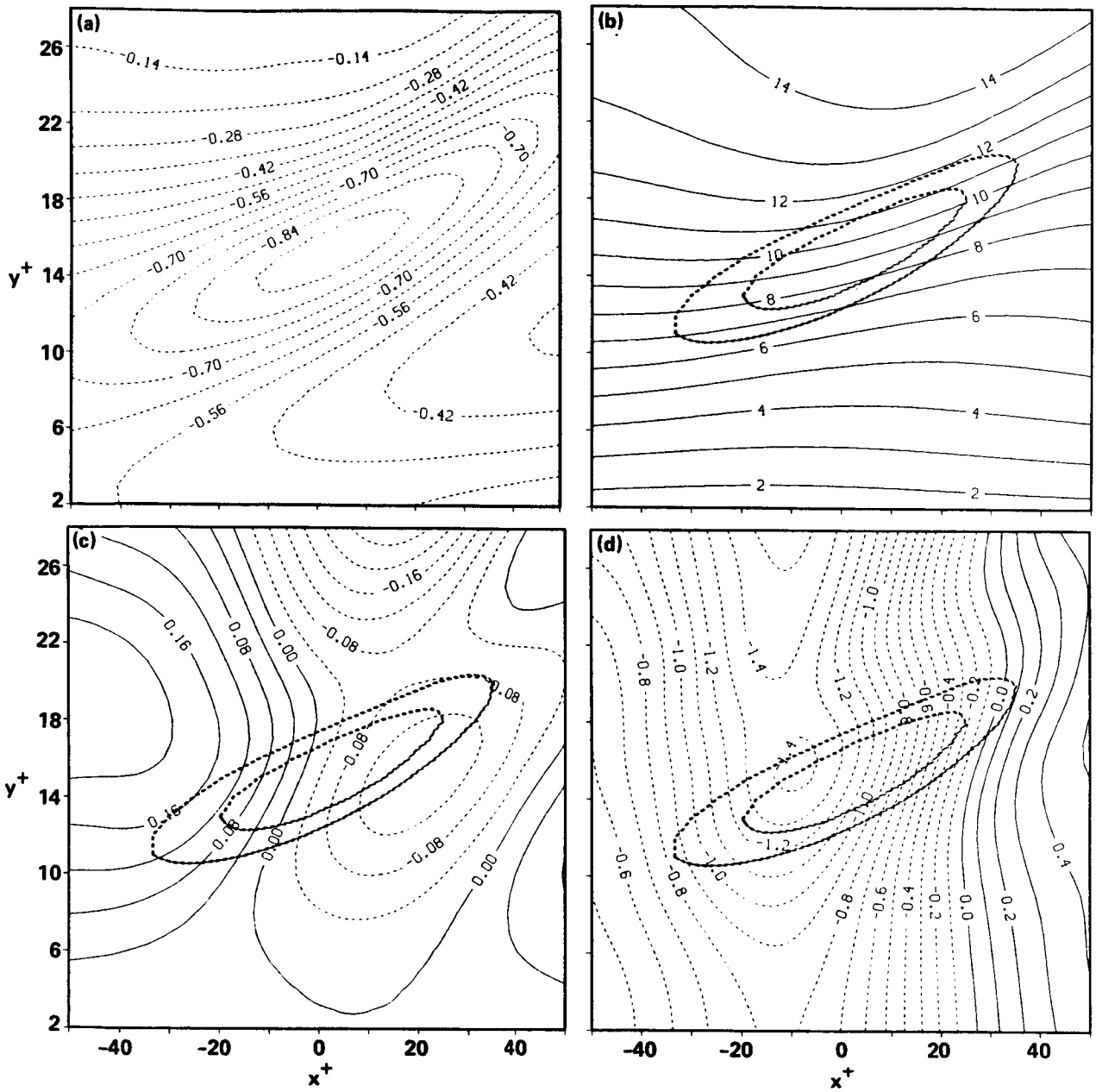

FIGURE 2. Educed turbulence structures centered at $y^+ = 15$. Note that the y-scales are stretched to reveal the details of the structures. (a) $< \omega_z >$; (b) $< u >$; (c) $< v >$; (d) $< p >$; (e) $< q_r^2 >$; (f) $-< u_r v_r >$; (g) $< p_r^2 >$; (h) $< S >=< \partial u/partialy > + < \partial v/\partial x >$; (i) $< P_S >= - < u_r v_r >< S >$; (j) $< P_N >= - < u_r^2 > \partial < u > /\partial x - < v_r^2 > \partial < v > /\partial y$; (k) $< P_T >=< P_S > + < P_N >$; (l) $< p >< S_{11} >$; (m) $< p >< S_{22} >$.

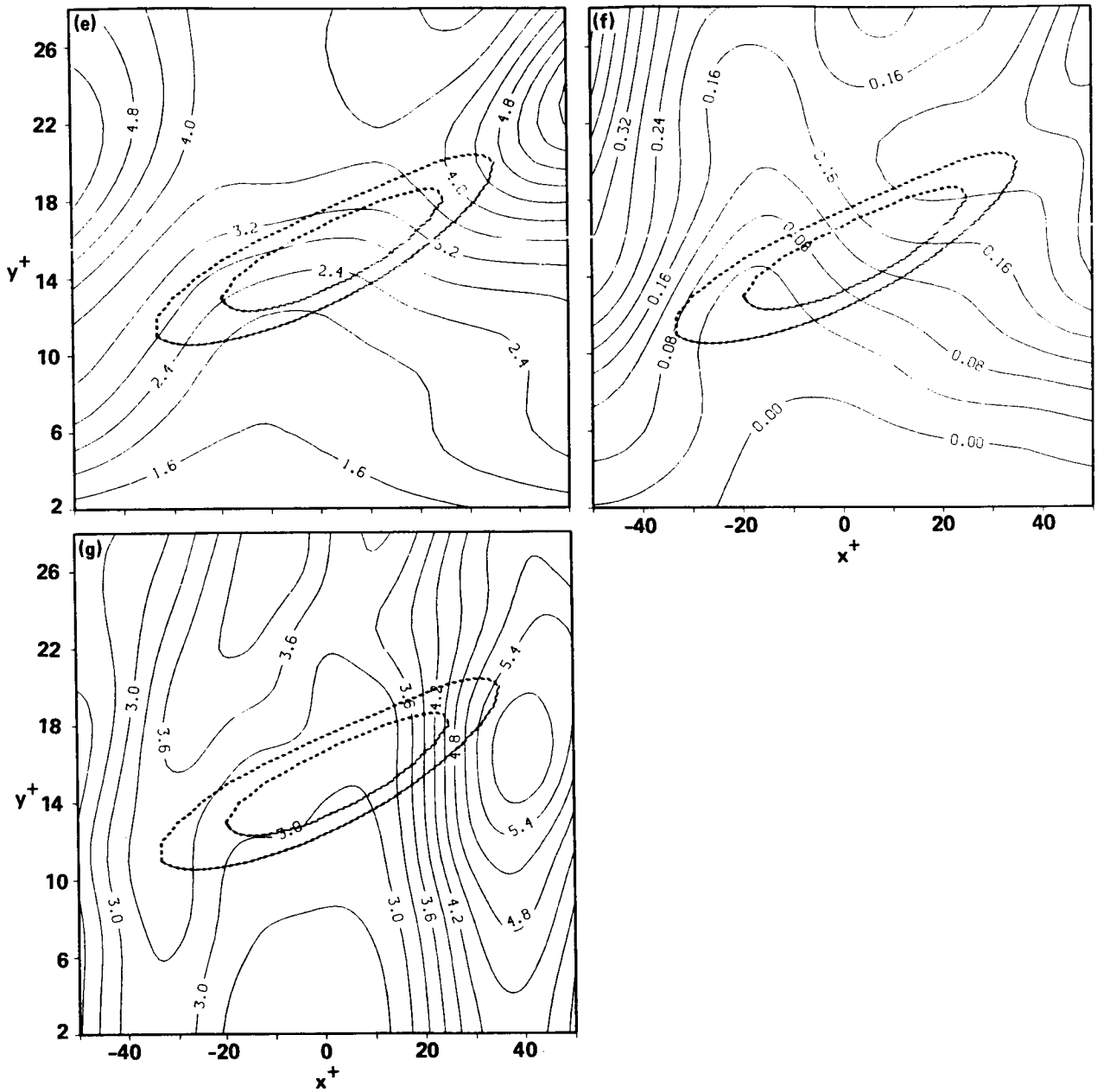

FIGURE 2. ... continued.

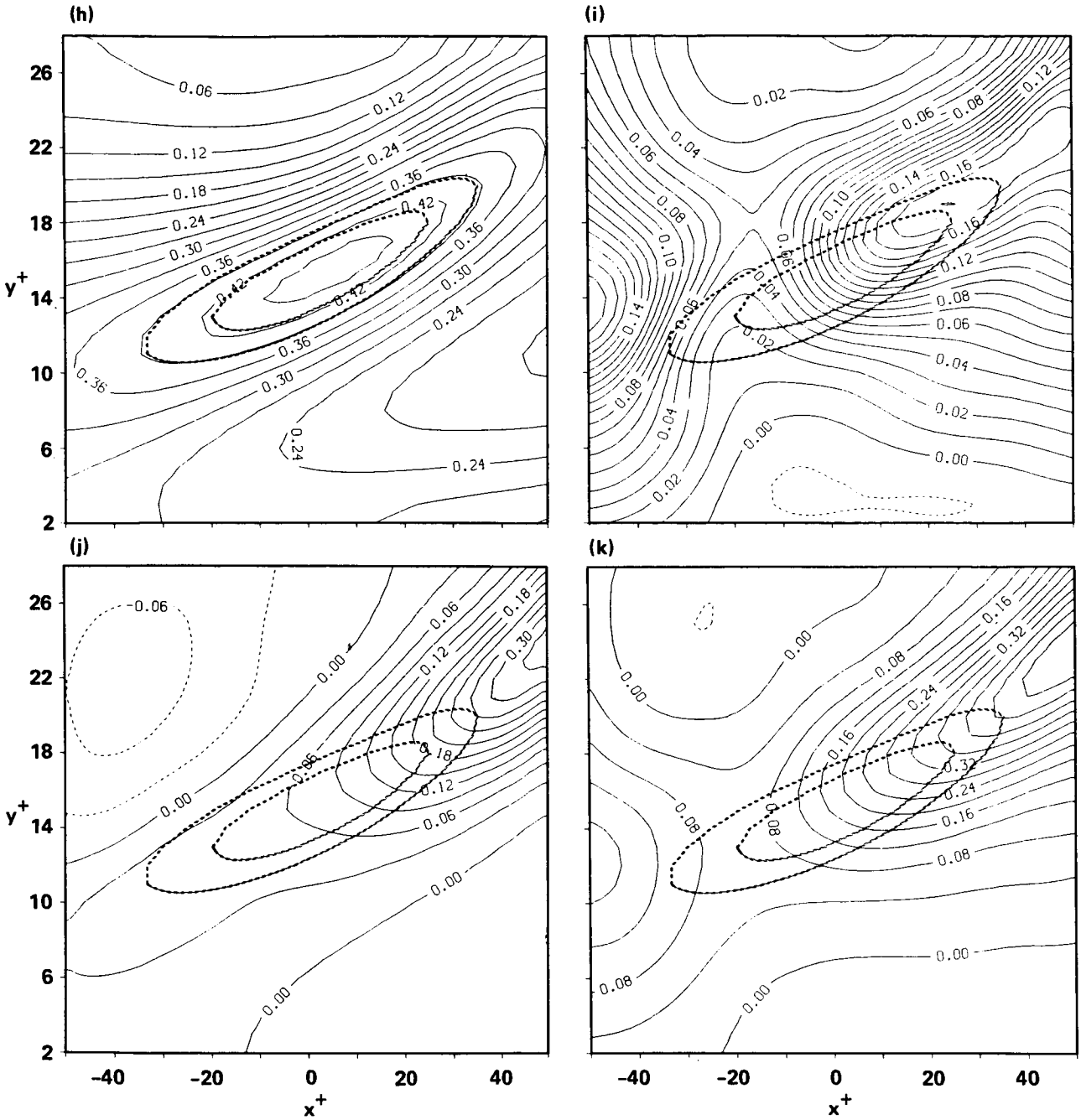

FIGURE 2. ... continued.

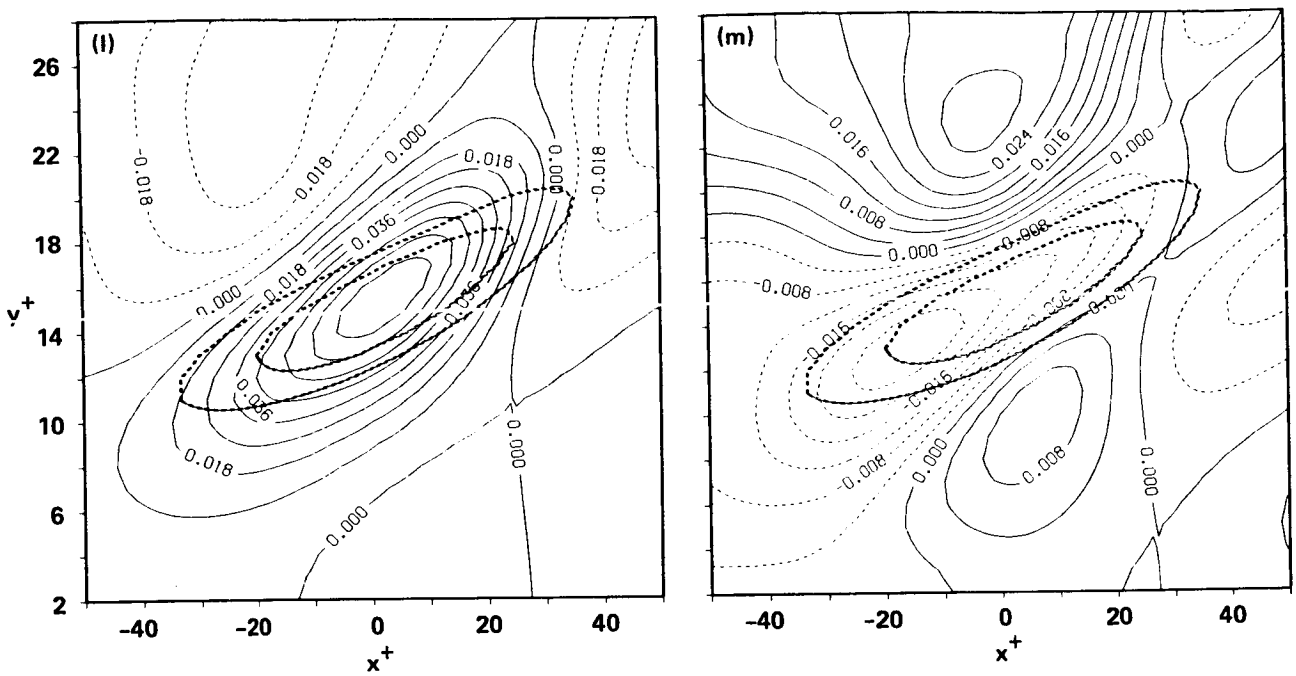

FIGURE 2. ... continued.

the opposite wall.

(3) Complete eduction on the basis of total vorticity $|\omega|$ rather than the spanwise vorticity ω_z.

(4) Address clearly the mechanisms of entrainment, mixing, production, intercomponent transport, enstrophy cascade and dissipation associated with the educed three-dimensional coherent structure.

(5) Educe other significant coherent structures and evaluate the dynamical role and significance of coherent structures in the three flows studied.

(6) Study the evolution of a turbulent hairpin vortex in a laminar boundary layer and a laminar channel flow with a velocity profile matching that of a turbulent flow. Study the same in a flow with laminar and turbulent homogeneous shear.

(7) Study the dynamics and evolution of an an artificially induced bursting coherent structure in fully turbulent channel flow and flat plate boundary layer.

B. Propagation velocities

The direct simulation data provide an excellent opportunity for determination of propagation velocities of pressure, velocity and vorticity perturbations in turbulent shear flows. In the case of the turbulent boundary layer or channel flow, in particular, varying values of propagation velocities have been reported in the literature. In addition to being of fundamental interest, the propagation velocity is of direct concern in understanding coherent structure topology and dynamics.

If instantaneous fields of simulation data are considered at two instants t_1 and t_2

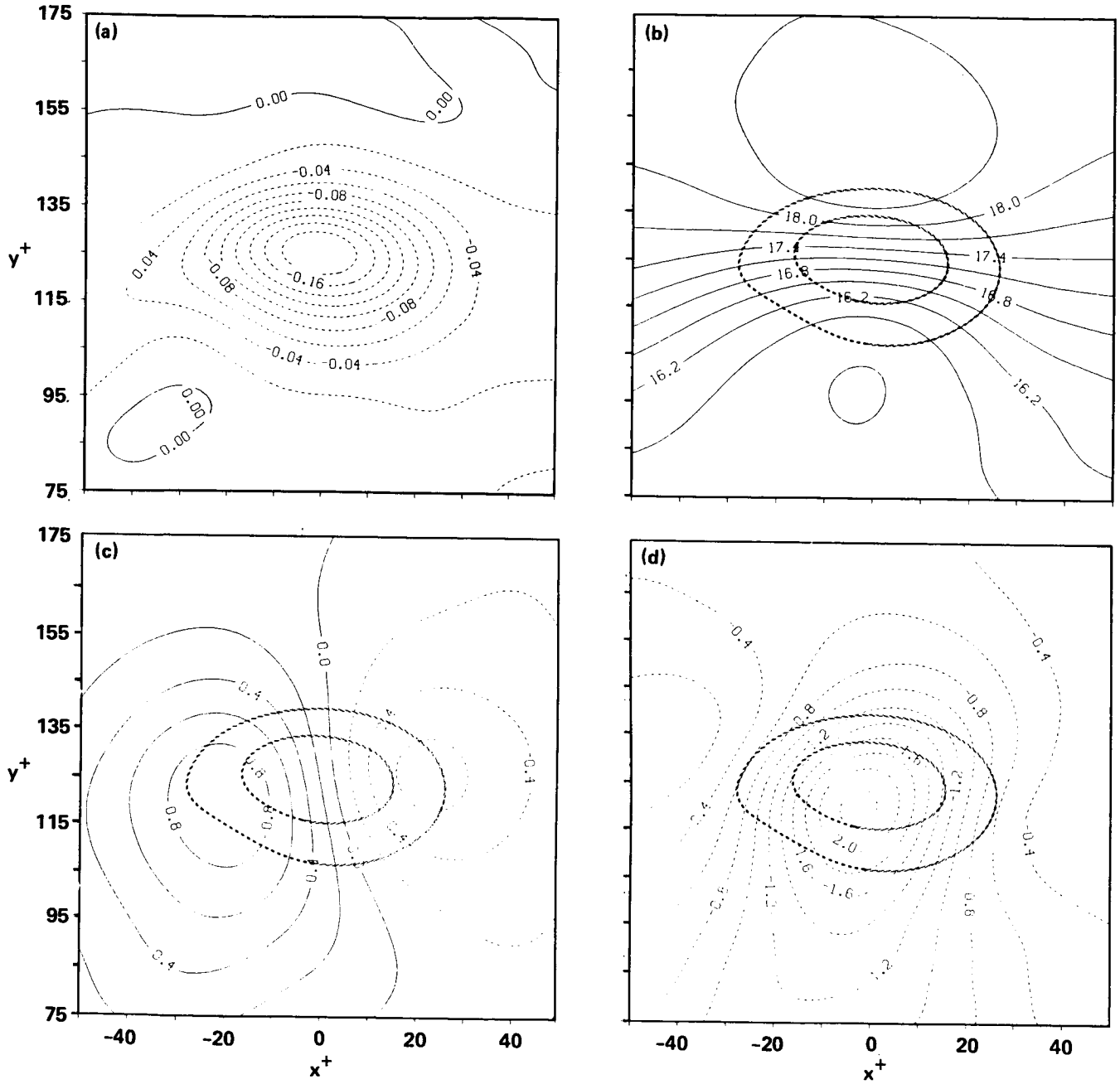

FIGURE 3. Educed turbulence structures centered at $y^+ = 125$. Note that the y-scales are stretched to reveal the details of the structures. (a) $< \omega_z >$; (b) $< u >$; (c) $< v >$; (d) $< p >$; (e) $< q_r^2 >$; (f) $-< u_r v_r >$; (g) $< p_r^2 >$; (h) $< S >=< \partial u/partialy > + < \partial v/\partial x >$; (i) $< P_S >= - < u_r v_r >< S >$; (j) $< P_N >= - < u_r^2 > \partial < u > /\partial x - < v_r^2 > \partial < v > /\partial y$; (k) $< P_T >=< P_S > + < P_N >$; (l) $< p >< S_{11} >$; (m) $< p >< S_{22} >$.

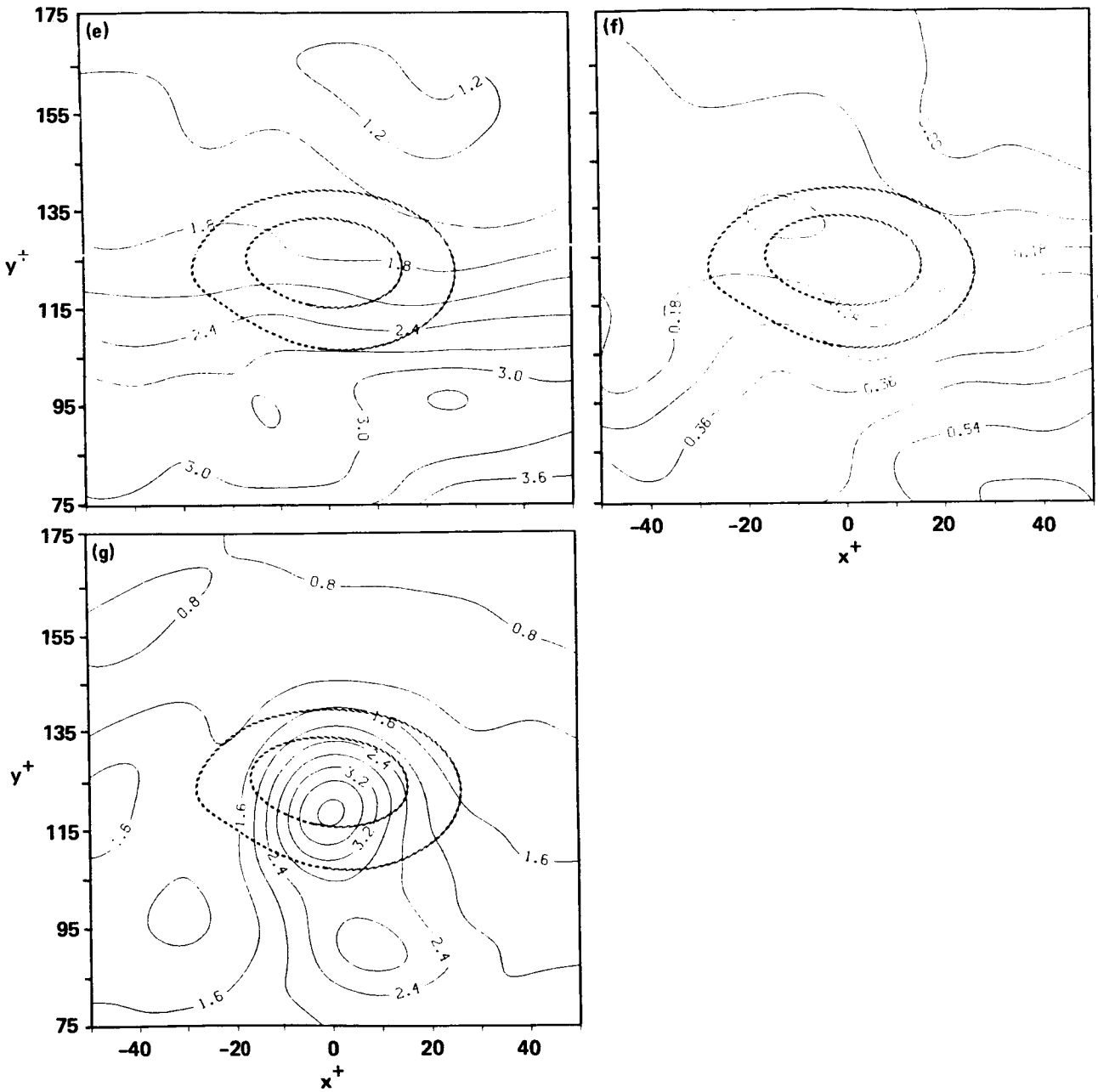

FIGURE 3. ... continued.

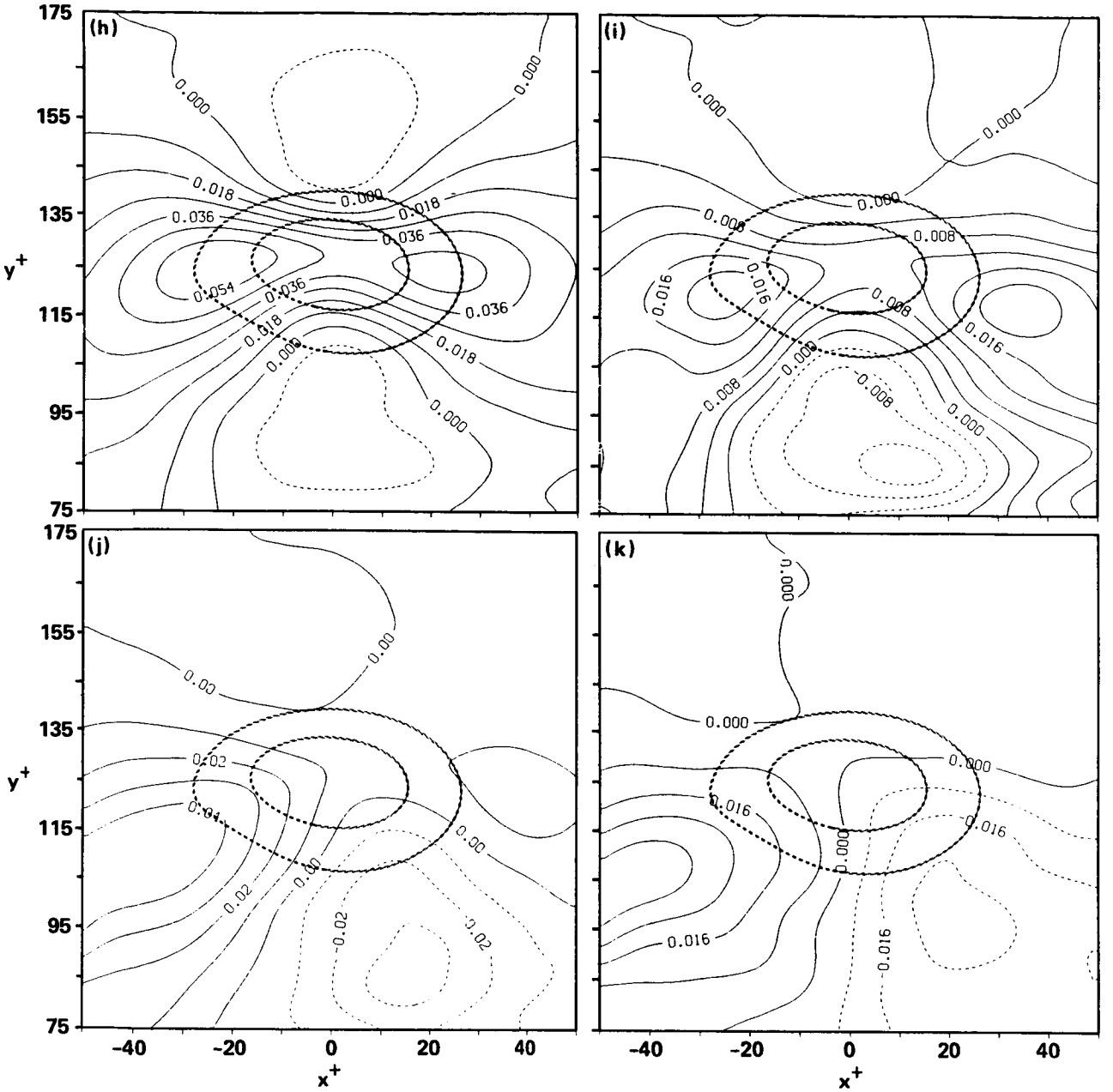

FIGURE 3. ... continued.

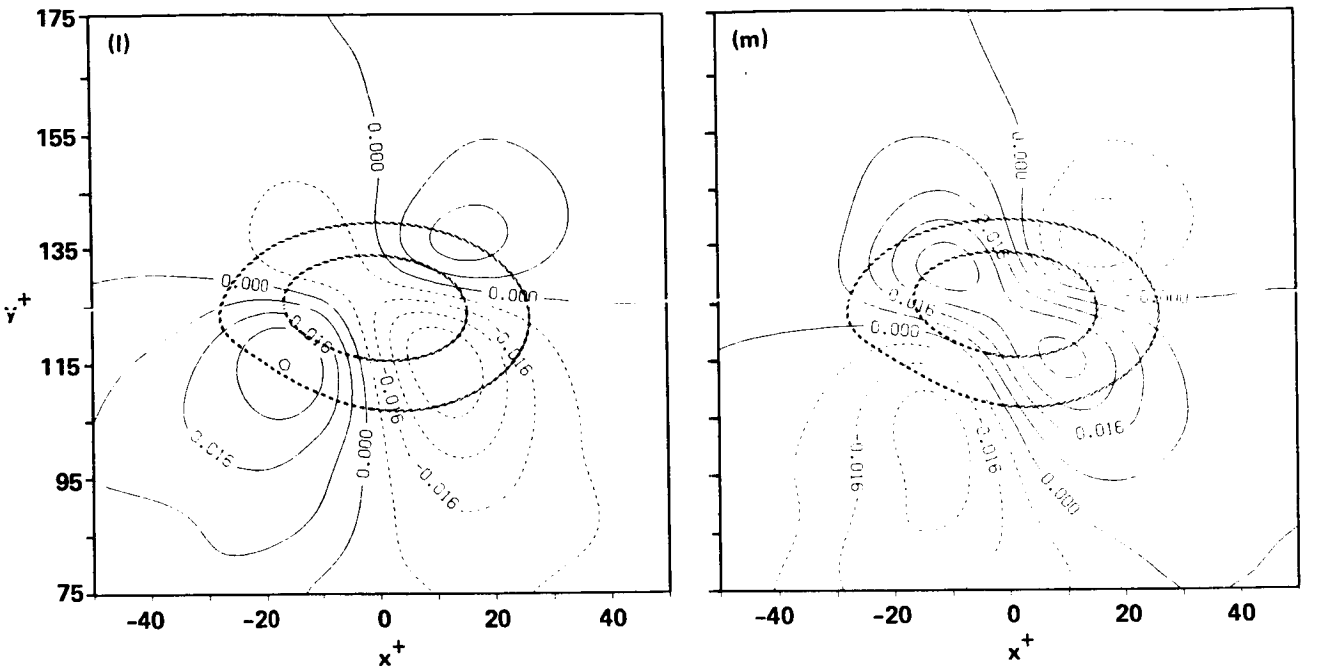

FIGURE 3. ... continued.

and they are cross-correlated, then from the locations $(\delta x_m, \delta y_m)$ of cross- correlation peak, one can obtain streamwise and transverse propagation velocities U_c, V_c as follows:

$$U_c = \frac{\delta x_m}{(t_2 - t_1)}$$

$$V_c = \frac{\delta y_m}{(t_2 - t_1)}$$

As a first step, we have determined values of U_c from streamwise correlations of velocity (u_i), pressure (p), and vorticity (ω_i) fields. Fig. 4a shows the profiles of U_c for u_i and p as functions of y, and Fig. 5a shows the profiles of U_c for vorticity (ω_i). Figs. 4b and 5b show the same profiles as functions of y^+.

It is surprising how closely the convection velocities for velocity and vorticity perturbations agree with each other. Moreover, these profiles closely agree with the mean velocity profile, being only slightly lower than mean velocity in the outer region, but being higher than the mean velocity near the wall. There are clear differences between the data presented here and those reported in literature. The convection velocity of pressure in the wall region is consistently higher than those of velocity and vorticity, indicating somewhat the elliptic nature of the pressure field.

Future extensions

(1) To determine V_c in addition to U_c. When correlation in (x and y) is used, the current value of U_c may be somewhat different from that found from the x-correlation alone.

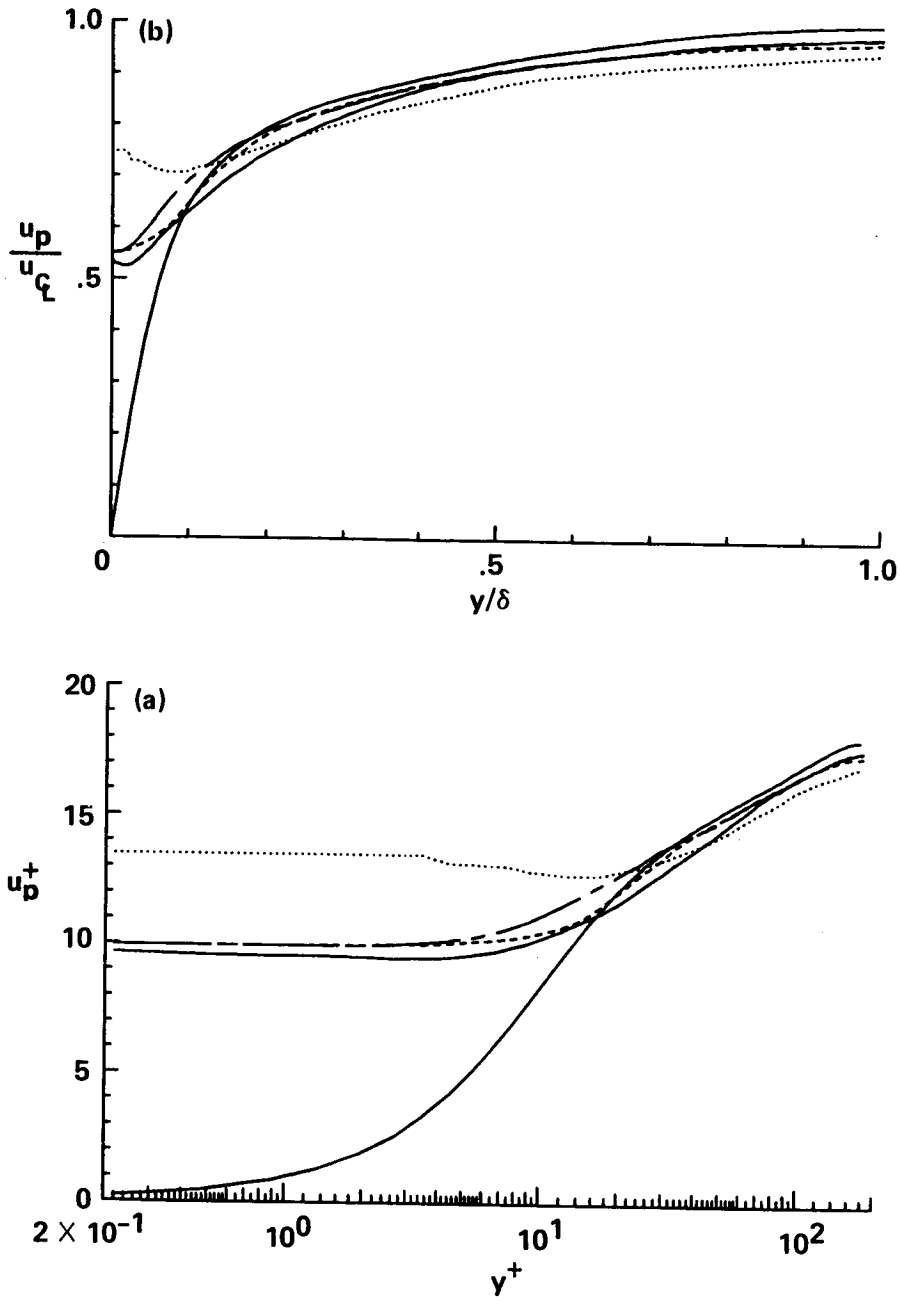

FIGURE 4. Propagation velocity for velocity and pressre (a) in global coordinate, (b) in wall coordinate: ——— , u; - - - - , v; — — — , w; ····· , p.

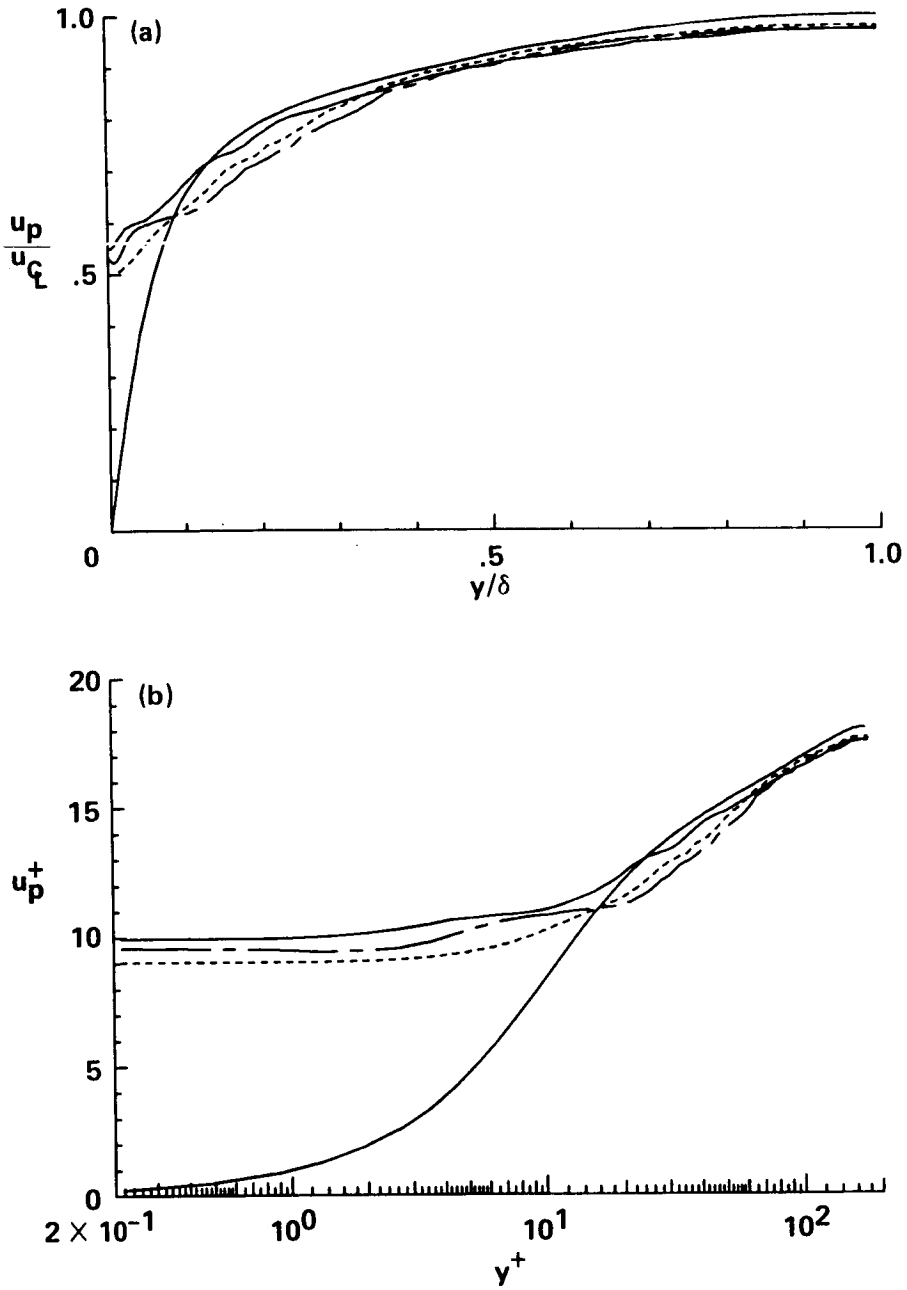

FIGURE 5. Propagation velocity for vorticity (a) in global coordinate, (b) in wall coordinate: ——— , ω_x; - - - - , ω_y; — — — , ω_z.

(2) Determine U_c and V_c for positive and negative ω_z separately.
(3) Determine U_c and V_c values for all variables in the two homogeneous shear flows.

C. Taylor hypothesis

The Taylor hypothesis of frozen turbulence is a common assumption in experimental turbulence for inferring spatial structure of turbulence from temporal data obtained by a stationary probe. It is also commonly invoked for inferring wave number spectrum from measured frequency spectrum as well as in measurements of dissipation and higher-order moments. While there have been extensive discussions of the limitation of the hypothesis, which were obviously known to Taylor himself, no direct test of this hypothesis has been possible yet. The direct numerical simulation databases allow us to make a thorough evaluation of this hypothesis for different flow variables as a function of shear rate.

The hypothesis assumes that

$$D_T\phi = (\frac{\partial}{\partial t} + U_T\frac{\partial}{\partial x})\phi = 0$$

where U_T is the Taylor advection velocity and ϕ can be any of the variables $\{u_i, p, \omega_i, c\}$. The value of U_T used in the literature has varied (Zaman & Hussain, 1981):

$U_T = U(y),$	mean velocity
$= u(x,y,z),$	local velocity
$= U_c(y),$	propagation velocity
$= u_f(x,y,z),$	filtered velocity

We have used the first, second and fourth in the 1987 CTR session. It is seen that both mean and rms values of $D_T\phi$ are small in the outer layer, except very close to the wall. Comparing instantaneous contours of $D_T\phi$ with the smoothed contours of u_i, ω_i, p, it is found that the departure from the hypothesis is not directly associated with large-scale structures.

Future extensions

(1) Compute vorticity fields using Taylor hypothesis and velocity fields, and compare with true vorticity fields.
(2) Determine which choice of U_T produces the minimum error in the use of the Taylor hypothesis.
(3) For situations when there are large values of $D_T\phi$, evaluate the various terms in the convective balance equations of ϕ. Determine which term (and hence which mechanism) produces the maximum contribution to the departure from $D_T\phi = 0$.

REFERENCES

CANTWELL, B. & COLES, D. 1983 An experimental study of entrainment and transport in the turbulent near wake of a circular cylinder . *J. Fluid Mech.*. **136**, 321.

HAYAKAWA, M. & HUSSAIN, A.K.M.F. 1985 Eduction of coherent structures in the turbulent plane wake. 5th Symposium on Turbulent Shear Flows, Cornell University, August 7-9, 1985.

HUSSAIN, A.K.M.F. 1980 Lecture Notes in Physics (ed. J. Jimenez), Springer-Verlag, 1980.

HUSSAIN, A.K.M.F. 1983 Coherent structures — Reality and Myth. *Phys. Fluids.* **26**, 2763.

HUSSAIN, A.K.M.F. 1986 Coherent structures and turbulence. *J. Fluid Mech.*. **173**, 303.

HUSSAIN, A.K.M.F. & ZAMAN, K.B.M.Q. 1980 Vortex pairing in a circular jet under controlled excitation. Part 2. Coherent structure dyanmics . *J. Fluid Mech.*. **101**, 449.

HUSSAIN, A.K.M.F. & ZAMAN, K.B.M.Q. 1985 An experimental study of organized motions in the turbulent mixing layer. *J. Fluid Mech.*. **159**, 85.

HUSSAIN, A.K.M.F., KLEIS, S.J. & SOKOLOV, M. 1980 A turbulent spot in an axisymmetric free shear layer. Part 2.. *J. Fluid Mech.*. **98**, 97.

KIM, J., MOIN, P. & MOSER, R.D. 1987 Turbulence statistics in fully developed channel flow at low Reynolds number. *J. Fluid Mech.*. **177**, 133.

LEE, M.J. & REYNOLDS, W.C. 1985 Numerical experiments on the structure of homogeneous turbulence, Report No. TF-24, Department of Mechanical Engineering, Stanford University, 1985.

METCALFE, R. HUSSAIN, A.K.M.F. & MENON, S. 1985 Coherent structures in a turbulent mixing layer: A comparison between direct numerical simulations and experiments, 5th Symposium on Turbulent Shear Flows, Cornell University, August 7-9, 1985.

MOIN, J. & KIM, J. 1982 Numerical investigation of turbulent channel flow . *J. Fluid Mech.*. **118**, 341.

ROGERS, M.R. & MOIN, P. 1987 The structure of the vorticity field in homogeneous turbulent flows. *J. Fluid Mech.*. **176**, 33.

SPALART, P. 1987 Direct simulation of a turbulent boundary layer up to R_θ = 1410. NASA Technical Memorandum 89407.

TENNEKES, H. & LUMLEY, J.L. 1972 A First Course in Turbulence, The MIT Press, 1972.

TSO, J. 1983 Ph.D Thesis, The Johns Hopkins University, 1983.

ZAMAN, K.B.M.Q. & HUSSAIN, A.K.M.F. 1981 Taylor hypothesis and large-scale coherent structures. *J. Fluid Mech.*. **112**, 379.

ZAMAN, K.B.M.Q. & HUSSAIN, A.K.M.F. 1984 Natural large-scale structures in the axisymmetric mixing layer. *J. Fluid Mech.*. **138**, 325.